

## DIAMOND - LIKE CARBON COATINGS FOR TRIBOLOGICAL APPLICATIONS

Bui Xuan Lam

University of Groningen, the Netherlands

(Manuscript Received on November 28<sup>th</sup>, 2007, Manuscript Revised June 27<sup>th</sup>, 2008)

**ABSTRACT:** *This paper presents studies on the morphology, mechanical and tribological properties of hydrogen-free diamond-like carbon (DLC) coatings deposited via magnetron sputtering under different bias voltages. Atomic force microscope (AFM), transmission electron microscope (TEM), Raman spectroscopy, nano-indentation and ball-on-disc tribotest were employed to characterize the deposited coatings. Diamond-like carbon coatings had very smooth surface with the roughness ( $R_a$ ) of less than 3.5 nm (for 1.2  $\mu\text{m}$  - thick coatings on Si wafer). Under high bias voltage, superhard coatings with hardness of more than 30 GPa were obtained. The self-lubrication mechanism of diamond-like carbon combined with smooth surface resulted in very low coefficients friction of less than 0.15. Magnetron sputtered diamond-like carbon show a big potential for tribological applications, especially, under dry or poorly lubricated conditions.*

**Keywords:** *magnetron sputtering, diamond-like carbon, bias voltage, hardness, roughness, tribology, graphitization*

### 1. INTRODUCTION

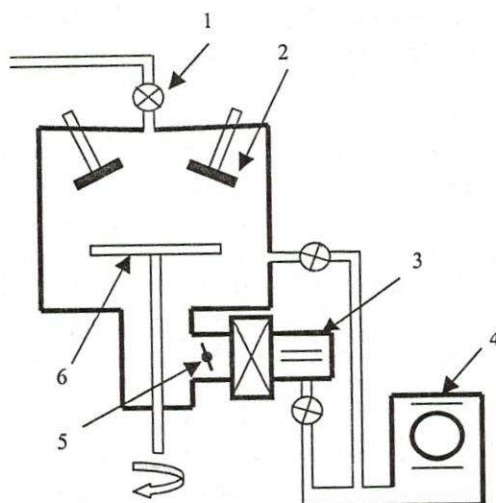
Carbon is one of the commonest elements throughout the Universe. The electronic configuration of carbon is written as  $1s^2 2s^2 2p^2$ . In the nature carbon is found as diamond, graphite and amorphous carbon. The name diamond-like carbon was first coined by Sol Aisenberg in 1971 to describe the hard carbon films that he prepared by direct deposition from low energy carbon ion beams [1]. Now, diamond-like carbon (DLC) is the name commonly accepted for hard carbon coatings which have similar mechanical, optical, electrical and chemical properties to natural diamond, but which do not have a dominant crystalline lattice structure. They are amorphous and consist of a mixture of  $sp^3$  (diamond) and  $sp^2$  (graphite) structures with  $sp^2$  bonded graphite clusters embedded in an amorphous  $sp^3$  bonded carbon matrix. So, the term "diamond-like" emphasizes a set of properties akin to diamond and, at the same time implies the absence of crystalline diamond order. DLCs are divided in to two broad categories: hydrogenated (a-C:H) and non-hydrogenated (a-C). The latter is sometimes called hydrogen-free DLC. DLC can be produced by various techniques and from various sources of carbon [2]. Comparing to hydrogenated DLC, in which hydrocarbon gases were employed as the source of carbon in the deposition process, hydrogen-free DLC shows advantages such as higher hardness, elastic modulus, and thus good wear resistance, lower coefficient of friction in humid environment, higher thermal stability, etc [3]. Hydrogen-free DLC coatings can be deposited by physical vapor deposition (PVD) techniques such as pulsed laser deposition [4] or filtered cathodic vacuum arc [5]. However, high residual stress of DLC coatings deposited by these techniques (up to 10 GPa) limits the coating thickness of 100-200 nm only.

In this study, thick (1.2  $\mu\text{m}$ ) and hard hydrogen-free DLC coatings were deposited via magnetron sputtering at high power density for a high deposition rate. The influence of deposition parameters on the surface morphology, mechanical and tribological properties of coatings was investigated.

## 2. EXPERIMENTAL

### 2.1. Deposition of DLC coatings

The DLC coatings were deposited using E303A magnetron sputtering system (PentaVacuum). The schematic diagram of the system is shown in fig. 1. The targets (99.999% pure graphite) locate about 100 mm above substrate holder. Co-sputtering of two targets was carried out. The system was equipped an 800 l/s cryogenic pump (3) and a 12 m<sup>3</sup>/h two stage rotary backing pump (4). The main chamber is rough pumped through a separate and direct path from the cryogenic pump. High vacuum pumping via the cryogenic pump is automatic once a suitable starting pressure has been obtained via the roughing pump. The vacuum system accepts the pressure in the main chamber to reach 10<sup>-7</sup> torr as a base pressure. The process pressure was kept constant by the butterfly valve (5). For all coatings, the process pressure was kept at 3 mTorr, the Ar flow was 50 sccm (standard cubic centimeter per minute). The coatings were deposited on 440C steel discs (55 mm in diameter and 5.5mm in thickness) and silicon wafer (100 mm in diameter and 0.45 mm in thickness, R<sub>a</sub> < 2 nm). The steel substrates were polished to the surface roughness of R<sub>a</sub>=60nm. The power density on graphite targets was 12 W/cm<sup>2</sup>. Before sputtering, the substrates were ultrasonic cleaned for 20 minutes in acetone then 10 minutes in ethanol. Plasma cleaning was applied for 30 minutes at RF bias of 300 V in order to remove oxide layer and contaminants on the surface of the substrates.



- |                   |                     |
|-------------------|---------------------|
| 1- Gas feed line  | 4- Rotary pump      |
| 2- Target         | 5- Butterfly valve  |
| 3- Cryogenic pump | 6- Substrate holder |

Figure 1. Diagram of E303A magnetron sputtering system

### 2.2. Characterization of DLC coatings

Coating thickness was measured using a laser profilometer (Wyko) through a sharp step. To make the step, a couple of thin marks making by marker were made on the surface of silicon substrate. After deposition, those marks were erased using acetone and the steps were formed. Surface morphology was investigated using Atomic Force Microscope (AFM,

Shimadzu SPM-9500J2). The surface roughness of coatings was calculated using the software combining with AFM over an area of  $2 \times 2 \mu\text{m}$ . Coating hardness was measured using Nano Indenter (XP) with a three sided pyramid-shaped Berkovich diamond indenter. The hardness was determined by CSM (continuous stiffness measurement) technique [6]. The indentation depths were set not to exceed 10 % of coating thickness to assure the accuracy [7]. Six indentations were made on each coating, and the average value was obtained. Microstructure of the coating was investigated by Raman spectroscopy (Renishaw) with 633nm lines of HeNe laser as the excitation source. Visually, the structure was observed using Transmission Electron Microscope (TEM, JEOL - JEM 2010). Tribological behavior was characterized by CSEM tribometer with ball on disk configuration in ambient environment (75% humidity,  $22^\circ\text{C}$ ). 100Cr6 steel ball with diameter of 6 mm was chosen as counter part. Applied load was set at 5 N for all tests.

### 3. RESULTS AND DISCUSSION

#### 3.1. Coating structure and morphology

Fig. 2 shows a typical Raman spectrum of DLC coating deposited via magnetron sputtering. The range of Raman shift was from  $850$  to  $2000 \text{ cm}^{-1}$ . A broad peak at about  $1530 \text{ cm}^{-1}$  with a shoulder at about  $1360 \text{ cm}^{-1}$  was observed. This broad peak was deconvoluted into two Gaussian bands at about  $1530 \text{ cm}^{-1}$  (Graphite or G peak) and  $1360 \text{ cm}^{-1}$  (Disorder or D peak) [8]. The ratio between the intensity of D peak and G peak ( $I_D/I_G$ ) of DLC coatings deposited under different bias voltages was taken and shown in fig. 3.

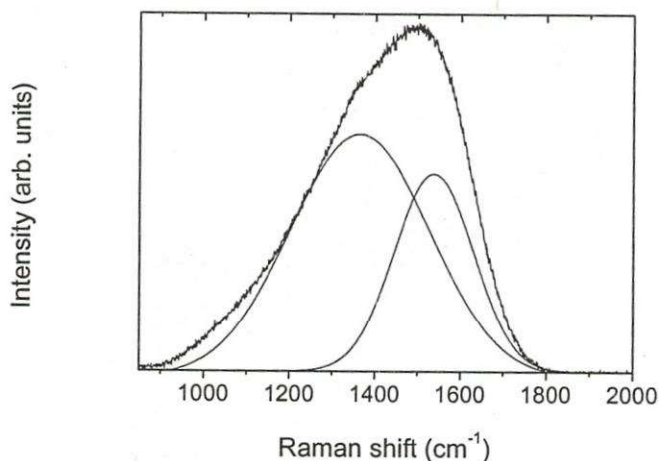


Figure 2. Raman spectrum of magnetron sputtered DLC coating

It is well known that the composition of  $\text{sp}^3$  in DLC is inversely proportional to  $I_D/I_G$  ratio [8]. From fig. 3, at bias voltage of  $-20 \text{ V}$ , the  $I_D/I_G$  ratio was 1.9. As bias voltage increased, the  $I_D/I_G$  ratio decreased. At  $-140 \text{ V}$  bias, the  $I_D/I_G$  ratio was 1.1 and it did not decrease with further increase of bias voltage. This indicated an increase of  $\text{sp}^3$  fraction in the DLC coating with increase of ion energy (here in term of negative bias voltage). The explanation for high  $\text{sp}^3$  fraction observed in highly biased coatings is the ion impingement and re-sputtering of carbon atoms from the graphite clusters. High bias voltage results in high energy of ion bombardment,

which hinders the surface diffusion thus the formation of graphite-like clusters. Also, at high bias voltage, re-sputtering strongly takes place. It should be noted that bonds of carbon atoms in graphite structure are weak therefore the carbon atoms in graphite clusters are easily dislodged from those. Consequently, the formation of graphite clusters in the coating is hindered. However, a maximum  $sp^3$  fraction can only be obtained at a certain range of energy thus a certain range of bias voltage. Excess of the energy (in this case when bias voltage of higher than -140 V is applied) does not result in more  $sp^3$  fraction in the coating. Understandably, excessive energy produces much heat in the coating leading to an increase in the temperature. High temperature promotes the graphitization, which results in the decrease of  $sp^3$  fraction.

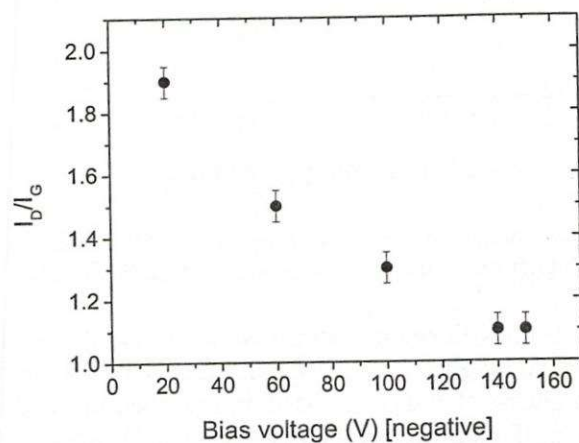


Figure 3.  $I_D/I_G$  ratio measured from DLC coatings deposited under different bias voltages

The amorphous structure of DLC can be seen from TEM image with a broad halo of diffraction pattern in fig. 4. Values of surface roughness  $R_a$  calculated from AFM analysis of coatings deposited under various bias voltages are shown in fig.5.

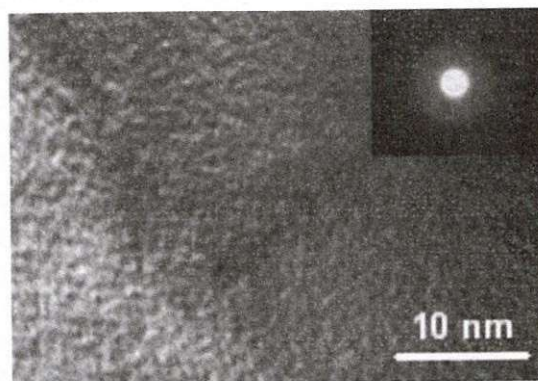
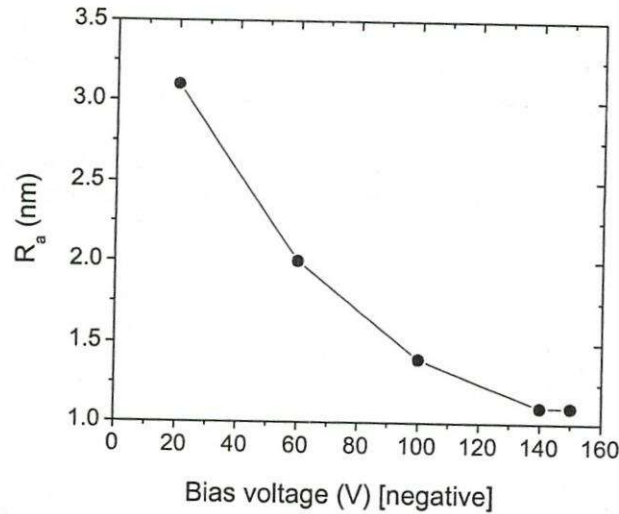


Figure 4. TEM image of DLC coating showing the amorphous nature with a broad halo observed from diffraction pattern



**Figure 5.** The influence of bias voltage on the surface roughness of DLC coatings: coatings deposited under higher bias voltage has smoother surface (lower  $R_a$ )

The  $R_a$  was as high as 3.1 nm with coating deposited under -20 V bias, as bias voltage was increased to -100 V, the surface roughness decreased drastically to 1.4 nm. Further increasing bias voltage, the surface roughness slightly decreased and reached the value of 1.1 nm at bias voltage of -140 V. After that, the surface roughness almost unchanged as further increasing bias voltage. This observation indicates that upon the energy of carbon ions reaches a critical level, the coating has a smoothest surface (minimum size of graphite clusters) and a further increase in the energy (in terms of bias voltage) does not result in smoother morphologies.

### 3.2. Hardness

Hardness and Young's modulus of the coatings as a function of bias voltage are illustrated in fig. 6. Since the hardness is proportional to the  $sp^3$  fraction in the coating, understandably, coatings deposited under higher bias voltage have higher hardness (due to higher  $sp^3$  fraction in the structure as studied in previous section). The hardness and Young's modulus increased from 16.6 to 32.2 GPa and 178.5 to 345.6 GPa, respectively, as the bias voltage increased from -20 to -140 V. After that, further increase of bias voltage did not result in a considerable increase in the hardness and Young's modulus. This is consistent with the observation on the  $sp^3$  fraction in the coatings from Raman results.

The plasticity during indentation deformation was used to evaluate the toughness (or load-bearing capability) of the coating [9]. Coating has higher plasticity possesses better toughness and the brittle fracture at high applied load can be avoided. The calculated plasticity was 43 % for the coating deposited under -150 V bias. Such plastic compliance is evaluated high for a hard coating compared to 10 % plastic deformation of superhard DLC coating deposited by pulsed laser [10], or absence of plasticity of superhard nanocomposites TiN/SiN<sub>x</sub> proposed by Veprék et al [11].

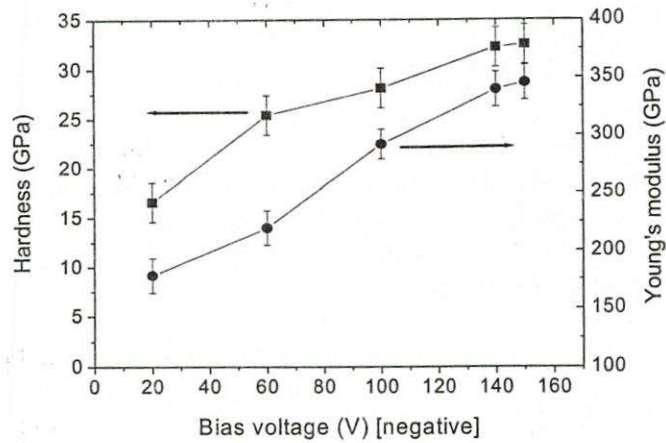


Figure 6. Hardness and Young's modulus of DLC coatings as a function of negative bias voltage

### 3.3. Tribological properties

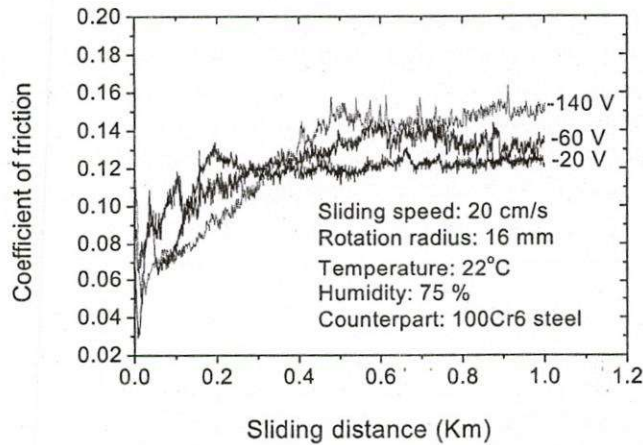
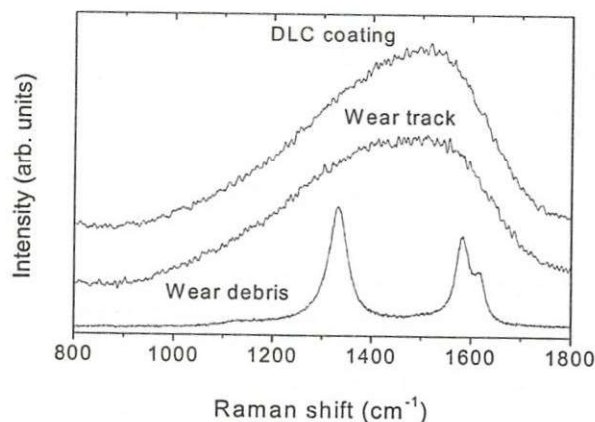


Figure 7. Coefficient of friction as a function of sliding distance with DLC coatings deposited under different bias voltages when sliding against 100Cr6 steel ball

Fig. 7 shows the coefficient of friction as a function of sliding distance of DLC coatings deposited under -20, -60 and -140 V bias. For all three coatings, at the beginning of the tests (several tens meters of sliding), the coefficient of friction reduced. This is due to a thin graphite-rich layer, which always exists on the surface of DLC. In humid air, this layer absorbs the moisture and becomes a good lubricant. With time, more moisture was absorbed leading to a decrease of coefficient of friction. However, after a short time this layer was removed and the coefficient of friction started to increase due to the surface-surface contact and the formation of wear particles. Coating deposited under higher bias voltage exhibited lower

friction due to a smoother surface. However, as the sliding distance was high enough, coating deposited under lower bias voltage exhibited lower coefficient of friction. Since the  $sp^2$  content in the coatings deposited under low bias voltage was higher, more graphite existed at the contact area. This combined with the graphite produced from the graphitization (the evidence of graphitization will be seen in the next paragraph) resulted in more lubricant at the contact area. The formation of more solid lubricant (compared to that of coatings deposited under higher bias voltage) compensated the effect of surface roughness leading to lower coefficients of friction observed. It should be noted that the graphite-rich lubrication layer is formed only after a certain sliding distance depending on the structure of the DLC coating (when other conditions are all the same). By the end of the tests, the coefficients of friction of all coatings came to stable values of 0.12, 0.13 and 0.15 for coatings deposited under -20, -60 and -140V bias, respectively. Such coefficients of friction are very low compared to that of other hard coatings, which are being used in engineering such as TiN, CrN, TiC, of which the coefficients of friction are 0.4 - 0.9 [12].

Fig.8 shows the Raman spectra of DLC coating (-140 V bias), the wear track on that coating after tribotest and the wear debris. The transformation of the coating structure from amorphous DLC to polycrystalline graphite in the wear debris can be observed by following the increase in the band width and the intensity of the Raman scattering near  $1580\text{ cm}^{-1}$ . A notable increase in the G (graphite) band of the Raman taken inside the wear track indicated the  $sp^3$  to  $sp^2$  phase transition occurring at the friction contacts on the DLC coating surface. From the visual observation and the Raman analysis of the wear track and wear scar, it was clear that graphite-like ( $sp^2$ ) was formed in the contact area between the DLC coating and the counterpart. This phase had low shear strength and was easily removed from the surface of DLC coating under stresses developed during the friction contact. The volume of the  $sp^2$  phase removed was small and some adhered to the surface of the ball forming a lubricious transfer layer. Larger volumes of the  $sp^2$  phase, which was produced as wear debris, were pushed to the side of the track and the scar. Fig. 9 presents a schematic of how this process may take place.



**Figure 8.** Comparison of Raman spectra of as deposited DLC coating (-140 V bias), wear track, and wear debris. The graphite-like structure is seen from wear debris and the graphitization is confirmed from the Raman spectrum taken on the wear track

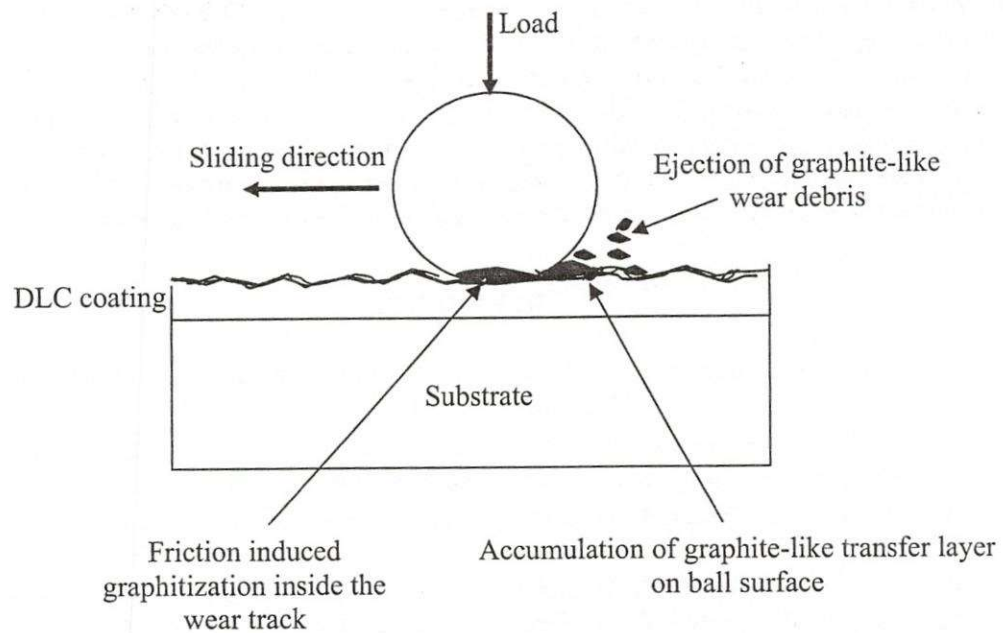


**Figure 9.** Schematic explanation of the formation of the graphite-like structure and the transfer layer accumulation observed after the wear test

#### 4. CONCLUSION

Hydrogen free DLC coatings deposited via magnetron sputtering have very high hardness (17-32GPa) and low friction (<0.15 under dry sliding condition against steel counterparts). Such properties are ideal for engineering applications.

The negative bias voltage strongly influences on the structure, thus mechanical and tribological properties of the coatings. An increase in substrate bias voltage results in more  $sp^3$  content (thus higher hardness) and smoother morphology. However, very high bias voltages (more than -140V) do not bring a further increase in  $sp^3$  content and smoothness of the coatings.

Coatings deposited under lower bias voltage exhibit lower coefficient of friction. The  $sp^3 \rightarrow sp^2$  transition (the graphitization) during the tribological operation is one of the major mechanisms driving the low friction of DLC coatings.

### MÀNG PHỦ CHỐNG MÒN CACBON GIỐNG KIM CƯƠNG

**Bùi Xuân Lâm**

Viện nghiên cứu vật liệu mới Hà Lan – Trường Đại học Groningen, Hà Lan

**TÓM TẮT:** Bài báo trình bày những nghiên cứu về bề mặt, cơ tính và các tính chất ma sát của màng cacbon giống kim cương không chứa hydro được phủ bằng kỹ thuật phun có từ trường tăng cường với các thế điện khác nhau trên vật cần phủ. Kính hiển vi cảm ứng lực



nguyên tử (AFM), kính hiển vi điện tử TEM, phổ Raman, thiết bị đo độ cứng nano và thiết bị đo ma sát với cấu hình bi trượt trên đĩa được sử dụng để xác định cấu trúc và tính chất của màng. Màng cacbon giống kim cương có bề mặt rất nhẵn với độ nhám  $R_a < 3,5$  nm (phủ trên Si với màng có độ dày 1,2  $\mu\text{m}$ ). Ở thế điện cao trên vật cần phủ, màng thu được là siêu cứng với độ cứng hơn 30 GPa. Cơ chế "tự bôi trơn" của cacbon giống kim cương cộng với bề mặt có độ nhẵn cao làm cho hệ số ma sát của màng rất bé ( $< 0,15$ ). Màng cacbon giống kim cương phủ bằng kỹ thuật phun có từ trường tăng cường có tiềm năng ứng dụng rất lớn trong kỹ thuật đặc biệt cho các chi tiết chịu mài mòn trong điều kiện bôi trơn kém hoặc không có bôi trơn.

## REFERENCES

- [1]. J. Angus, Diamond-like hydrocarbon and carbon films, *In Diamond and diamond like films and coatings*, p173, NewYork, (1991).
- [2]. Y. Catherine, Preparation techniques for diamond-like carbon, *In Diamond and diamond like films and coatings*, p193, NewYork (1991).
- [3]. Y. Lifshitz, Diamond-like carbon- present status, *Diamond and Related Materials* 8 (1999)1659-1676
- [4]. A.A Voevodin, M.S. Donley, Review: Preparation of amorphous diamond-like carbon by pulsed laser deposition: a critical review, *Surface and Coatings Technology* 8, 2199-213, (1996).
- [5]. X.Shi, L.K Cheah, B.K. Tay, Spectroscopic ellipsometry of tetrahedral amorphous carbon prepared by filtered cathodic vacuum arc technique, *Thin Solid Film* 312, 160-169, (1998).
- [6]. G.M. Pharr, Measurement of mechanical properties by ultra-low indentation, *Materials Science and Engineering* A253, 151-159, (1998).
- [7]. S. Veprék, The search for novel, superhard materials, *Journal of Vacuum Science Technology* A17(5), 2401-2420, (1999).
- [8]. S. Zhang, X.T. Zeng, H. Xie, P. Hing, A phenomenological approach for the  $I_D/I_G$  ratio and  $sp^3$  fraction of magnetron sputtered a -C films, *Surface and Coatings Technology* 123, 256-260, (2000).
- [9]. A.A. Voevodin, J.S. Zabinski, Load-adaptive crystalline-amorphous nanocomposites, *Journal of Materials Science* 33, 319-327, (1998).
- [10]. A.A. Voevodin, M.S. Donley, J.S. Zabinski, J. E. Bultman, Mechanical and tribological properties of diamond-like carbon coatings prepared by pulsed laser deposition, *Surface and Coatings Technology* 76-77, 534-539, (1995).
- [11]. S.Veprék, S. Reiprich, A concept for the design of novel superhard coatings, *Thin Solid Films* 268, 64-71, (1995).
- [12]. K. Hormberg, A. Matthews, Coatings tribology, *Tribology series* 28, (1994).